Multiple-Subcarrier Modulation for Nondirected Wireless Infrared Communication

Jeffrey B. Carruthers, *Member, IEEE,* and Joseph M. Kahn, *Member, IEEE*

Abstract—**We examine multiple-subcarrier modulation (MSM) schemes for wireless infrared digital communication in the indoor environment. Intensity modulation with direct detection (IM/DD) is employed, which results in equivalent baseband channels with a nonnegativity constraint on the input. The power efficiencies of modulation schemes are compared at 30 Mb/s and 100 Mb/s over an ensemble of experimentally determined multipath channels. Carrier selection and power shaping are examined as methods for improving MSM performance. It is found that MSM schemes can allow operation at higher data rates than single-carrier modulation schemes without equalization. Moreover, MSM schemes can be more bandwidth-efficient and also can provide a simple and flexible method for multiple access to the channel. However, they are not as power efficient as single-carrier schemes, and this will limit their use to applications which are not power limited.**

I. Introduction

NONDIRECTED infrared light is being examined as an alternative to radio for wireless indoor local area networks [1]–[4]. Although nondirected links using intensity modulation with direct detection (IM/DD) are immune to fading [2], multipath dispersion is still present since the light can arrive at the receiver via multiple paths of different lengths. High-speed, single-carrier modulation schemes, such as on–off keying (OOK) and L-pulse-position modulation, are wideband signals and suffer from intersymbol interference (ISI) due to the multipath dispersion when the symbol rate exceeds about 10 Mbaud. In multiple-subcarrier modulation (MSM),[1] the symbol rate of each subcarrier is reduced relative to that of a single carrier with the same total bit rate. Hence, each subcarrier becomes a narrowband signal, and since it experiences little distortion the receivers need not employ equalization. Also, MSM allows for multiple simultaneous users of the channel through allocation of the subcarriers to individual users (i.e., frequency-division multiplexing), and, hence, receivers need not process the aggregate link rate. Finally, MSM techniques can be more bandwidth efficient[2] than single-carrier modulation schemes, which will reduce the electrical bandwidth requirement of the receiver.

Manuscript revised November 1995. This work was supported by the National Sciences Foundation under Grant ECS-9 408 957 and the Natural Science and Engineering Research Council of Canada. This paper was presented in part at GLOBECOM'94, San Fransisco, CA, December 1994.

The authors are with the Department of Electrical Engineering and Computer Sciences, University of California at Berkeley, CA 94720 USA.

Publisher Item Identifier S 0733-8716(96)02523-1.

[1] MSM is referred to as subcarrier multiplexing (SCM) in fiber-optics literature.

[2] The electrical bandwidth of the modulation scheme does not greatly affect the potentially much wider optical bandwidth of the transmitted signal.

While nondirected propagation alleviates the need for physical alignment between transmitter and receiver,[3] a major drawback of this approach is the signal distortion caused by reflections from ceilings, walls, and other objects. To evaluate the possible impact of multipath distortion on high-speed infrared links, we make use of the experimental characterization of about 90 channels in five offices and conference rooms [2]. During all measurements, the receiver was placed at desk height and pointed upwards. To form line-of-sight (LOS) configurations, the transmitter was placed near the ceiling and pointed straight down, while for diffuse configurations, it was placed at desk height and pointed straight up. Shadowed LOS and diffuse configurations were formed by having a person stand next to the receiver so as to block the dominant reception path.

This paper will examine the performance and design of MSM schemes and compare them to single-carrier schemes in their power efficiency and robustness. Section II presents a channel model and compares that channel to the wireless radio channel and to optical-fiber systems using intensity-modulated lasers. A model for representing both single-carrier and MSM schemes is given in Section III, along with a method for calculation of the probability of error. The power efficiency of each modulation scheme is outlined in Section IV. Methods for improving the performance of MSM schemes are presented and evaluated in Section V, and the application of MSM to multi-user systems is discussed in Section VI. Concluding remarks can be found in Section VII.

II. Nondirected Infrared Channels

The modeling of nondirected infrared channels with IM/DD is illustrated in Fig. 1. The transmitted waveform $X(t)$ is the instantaneous optical power of the infrared emitter. The received waveform $Y(t)$ is the instantaneous current in the receiving photodetector, which is proportional to the integral over the photodetector surface of the total instantaneous optical power at each location. The channel can be modeled as a baseband linear system, with input power $X(t)$, output current $Y(t)$, and an impulse response $h(t)$, which is fixed for a given arrangement of transmitter, receiver, and intervening reflectors [2].

In many applications, nondirected infrared links are operated in the presence of intense infrared and visible background light. It is possible to reduce this received ambient light by optical bandpass or longpass filtering, but this background

[3] The transmitter and receiver do not have to be aligned since the transmitter uses a wide-angle beam and the receiver has a wide field-of-view.

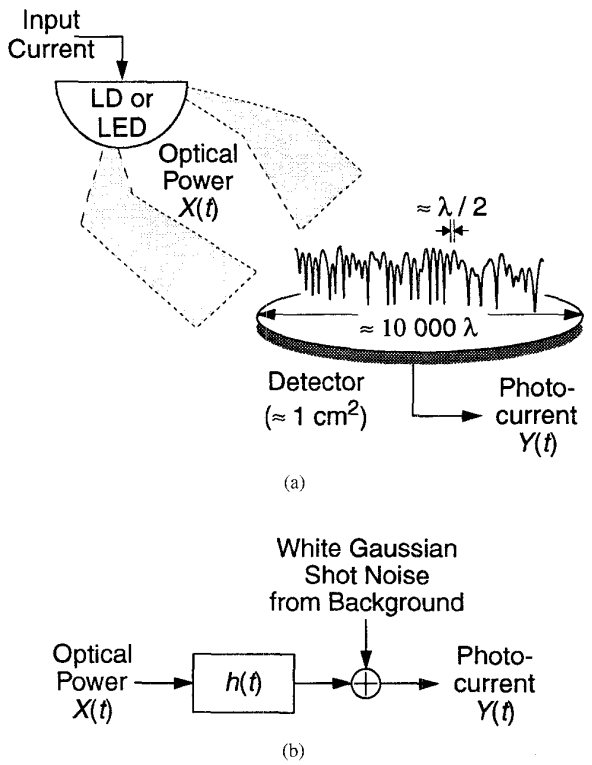

Fig. 1. Modeling nondirected infrared channels with intensity modulation and direct detection. (a) The received optical electric field generally exhibits spatial variation of magnitude and phase on the scale of a wavelength. The photocurrent is proportional to the integral over the detector surface of the optical power. (b) The channel can be modeled as a fixed, linear, baseband system with input $X(t)$, output $Y(t)$, impulse response $h(t)$, and additive white Gaussian noise.

light still adds a white, nearly Gaussian, shot noise $n(t)$ that is the limiting factor in the signal-to-noise ratio (SNR) of a well-designed receiver. Our channel model is summarized by

$$Y(t) \triangleq X(t) \otimes h(t) + n(t) \tag{1}$$

where $\otimes$ denotes convolution. We note that $H(0) = \int_{-\infty}^{\infty} h(t)\,dt$ is proportional to the optical path gain, i.e., the ratio of received average optical power to transmitted average optical power.

A. Comparison to Wireless Radio Channels

Temporal variation of the impulse response is a significant phenomenon of indoor radio communication. However, it is not a concern here because of the large, square-law photodetector. This detector results in the elimination of fading and makes the impulse response sensitive only to movements on the order of at least several centimeters. Estimating a maximum speed of 10 m/s for indoor objects, the impulse response can only change significantly in several milliseconds. Hence, at rates of several million b/s, as are considered here, the channel can be considered fixed over the duration of thousands of bits.

As in linear electrical or radio channels with additive noise, the SNR is proportional to $|X(t)|^2$. However, IM channels differ from conventional channels because the channel input $X(t)$ represents power. Thus, $X(t)$ cannot be negative and the average optical power is proportional to a time integral of $X(t)$

$$P_{\text{avg}} = \lim_{T\to\infty} \frac{1}{2T} \int_{-T}^{T} X(t)\,dt \tag{2}$$

rather than the usual $|X(t)|^2$, which is appropriate when $X(t)$ represents amplitude.

B. Comparison to Optical Fiber Channels

Two significant problems encountered with using intensity-modulated lasers to transmit subcarrier signals on optical fiber are clipping and intermodulation distortion (IMD) [5]. Clipping occurs in lightwave systems because, when the number of subcarriers is very large, the DC bias required to completely eliminate clipping may become very large. An improvement in system performance can be obtained by an increase in the modulation index beyond the onset of clipping, despite the fact that the clipping induces nonlinear distortion. The small number of subcarriers also implies that IMD should not be a significant problem. IMD can be eliminated, if necessary, by transmitting each subcarrier using a separate optical source.

III. MSM System Definition

We will proceed by first outlining the form of the transmitted signal and of the receiver, and then evaluating the probability of error in terms of the signal and noise powers.

A. Transmitted Signal

The binary input data stream is separated into M separate data streams which are then transmitted using N subcarrier frequencies. The data streams will be modulated in I and Q pairs onto the subcarrier frequencies, except in the case $N = 1$, for which there will be a single (usually baseband) subcarrier. Hence,

$$M = \begin{cases} 2N, & N > 1 \\ 1, & N = 1. \end{cases} \tag{3}$$

Now, each data stream m will have a symbol rate $1/T$ and a symbol set of size L_m. Hence, the aggregate bit rate is $R_b = 1/T \sum_1^M \log_2(L_m)$. We will denote by $a_{m,k}$ the symbol transmitted on data stream m at a delay kT. Each data stream m is defined by two pulse shapes $b_m^+(t)$ and $b_m^-(t)$ and a power coefficient P_m. Using the notation $\mu(x) \triangleq \max(x, 0)$, we can write the transmitted signal thus

$$X(t) \triangleq DC(T, \vec{b}^+, \vec{b}^-, \vec{P}) + \sum_{k=-\infty}^{\infty} \sum_{m=1}^{M} P_m \cdot \{\mu(a_{m,k}) \cdot b_m^+(t - kT) + \mu(-a_{m,k}) \cdot b_m^-(t - kT)\} \tag{4}$$

where DC is the offset required to ensure that $X(t)$ is always nonnegative and

$$a_{m,k} \in \left\{ \frac{\pm 1}{L_m - 1}, \frac{\pm 3}{L_m - 1}, \cdots, \pm 1 \right\}. \tag{5}$$

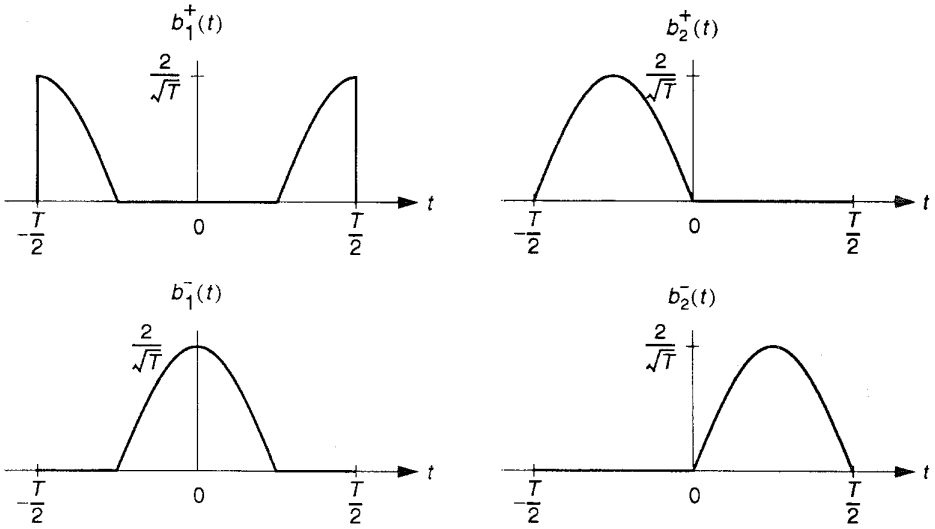

Fig. 2. Clipped 1–4 QAM signal set with carrier frequency $1/T$. On each time interval T, we send one of $\{b_1^+(t)+b_2^+(t), b_1^+(t)+b_2^-(t), b_1^-(t)+b_2^+(t), b_1^-(t)+b_2^-(t)\}$ which encode the four input data-symbol pairs $\{11, 10, 01, 00\}$, respectively. The matched-filter receiver is identical to a receiver designed for unclipped 4-QAM signals.

For signals of the form (4), the average optical power transmitted is thus

$$P_{\text{avg}} = DC(T, \vec{b}^+, \vec{b}^-, \vec{P}) + \frac{1}{T}\sum_{m=1}^{M} \cdot \left\{ \frac{P_m L_m}{2(L_m - 1)} \int_{-\infty}^{\infty} (b_m^+(t) + b_m^-(t))\, dt \right\}. \quad (6)$$

Let us see how the specific classes of modulation schemes fit into the framework provided by (4).

B. DC-Offset QAM

For quadrature amplitude modulation (QAM) signals using DC-offsetting, we denote the I and Q pulse shapes at subcarrier frequency f_n by $x_n(t)$ and $y_n(t)$

$$X_{\text{QAM}}(t) = DC + \sum_{k=-\infty}^{\infty}\sum_{n=1}^{N} A_n\{u_{n,k} \cdot x_n(t - kT) + v_{n,k} \cdot y_n(t - kT)\}. \quad (7)$$

This can be referred back to (4) by the associations

$$\begin{pmatrix} a_{(2n),k} \\ a_{(2n-1),k} \end{pmatrix} = \begin{pmatrix} u_{n,k} \\ v_{n,k} \end{pmatrix} \quad \text{and}$$
$$\begin{pmatrix} b_{2n}^+(t) & b_{2n}^-(t) \\ b_{2n-1}^+(t) & b_{2n-1}^-(t) \end{pmatrix} = \begin{pmatrix} x_n(t) & -x_n(t) \\ y_n(t) & -y_n(t) \end{pmatrix} \quad (8)$$

and by letting $P_{2n} = P_{2n-1} = A_n$. Since the pulse shapes $x_n(t)$ and $y_n(t)$ will be symmetric about zero, we will have the transmit power $P_{\text{avg}} = DC$, where DC is determined[4] by the power coefficients A_n and the particular shapes of $x_n(t)$ and $y_n(t)$.

[4]This is done either by inspection or, where necessary, an exhaustive search of data sequences.

C. "Clipped" QAM

It is also possible to use QAM signals on the IM/DD channel without adding a DC offset. This is done by half-wave rectifying, or "clipping" each subcarrier, as follows:

$$X_{\text{clip}}(t) = \sum_{k=-\infty}^{\infty}\sum_{n=1}^{N} A_n\{\mu(u_{n,k} \cdot x_n(t - kT)) + \mu(v_{n,k} \cdot y_n(t - kT))\} \quad (9)$$

where we make the associations

$$\begin{pmatrix} a_{(2n),k} \\ a_{(2n-1),k} \end{pmatrix} = \begin{pmatrix} u_{n,k} \\ v_{n,k} \end{pmatrix} \quad \text{and}$$
$$\begin{pmatrix} b_{2n}^+(t) & b_{2n}^-(t) \\ b_{2n-1}^+(t) & b_{2n-1}^-(t) \end{pmatrix} = \begin{pmatrix} \mu(x_n(t)) & \mu(-x_n(t)) \\ \mu(y_n(t)) & \mu(-y_n(t)) \end{pmatrix} \quad (10)$$

and by letting $P_{2n} = P_{2n-1} = A_n$. No DC offset is required since $\mu(\cdot)$ is nonnegative. An example of a clipped QAM subcarrier is shown in Fig. 2.

D. PAM

For pulse amplitude modulation (PAM), the transmitted signal will be

$$X_{\text{PAM}}(t) = DC + \sum_{k=-\infty}^{\infty} P_1 \cdot a_{1,k} \cdot r(t - kT) \quad (11)$$

where the pulse shape is $r(t)$ and we make the associations $b_1^+(t) = r(t)$ and $b_1^-(t) = -r(t)$.

E. Receiver Design

The receive filter for data stream m is matched to the difference between the plus and minus signal shapes

$$g_m(t) \triangleq b_m^+(\tau_m - t) - b_m^-(\tau_m - t). \quad (12)$$

This choice is motivated by the discussion of multipulse correlation receivers in [6]; for PAM and QAM, it is the matched-filter receiver for the nondistorting channel. τ_m represent the time delays introduced by the channel and are chosen to maximize the eye opening. They are assumed to be zero for the purposes of the following development.

Let us develop a discrete-time representation of the system by writing

$$\begin{aligned} d_{j,i}^{+}(k) &\triangleq b_j^{+}(t) \otimes h(t) \otimes g_i(t)|_{t=kT} \\ d_{j,i}^{-}(k) &\triangleq b_j^{-}(t) \otimes h(t) \otimes g_i(t)|_{t=kT}. \end{aligned} \tag{13}$$

The contribution of data stream j to the decision device input for data stream i at time kT can be represented as

$$Y_{i,j}(k) \triangleq P_j\{\mu(a_{j,k})\, d_{j,i}^{+}(k) + \mu(-a_{j,k})\, d_{j,i}^{-}(k)\}. \tag{14}$$

Since the time reference is arbitrary, we will restrict our consideration to detection of the symbol $a_{i,0}$ through examination of $Y_i \triangleq \phi_i + \psi_i + \Gamma_i$, where

$$\begin{aligned} \phi_i &= n(t) \otimes g_i(t)|_{t=0}, \quad \text{(noise)} \\ \psi_i &= \sum_{k=-\infty}^{\infty} \sum_{j=1}^{M} (1 - \delta_k \delta_{ij}) Y_{i,j}(k), \quad \text{(interference)} \\ \Gamma_i &= Y_{i,i}(0). \quad \text{(signal)} \end{aligned} \tag{15}$$

The signals will be designed so that for the nondistorting channel response $h(t) = \delta(t)$, we have the interference $\psi_i = 0$, the noise $\phi_i \sim \mathcal{N}(0, \sigma^2)$, and signal $\Gamma_i = P_i a_{i,0}$ for all data streams i and for all possible data sequences.

F. Probability of Error Calculation

The probability of symbol error in data stream i, written P_e^i, will depend on the sequences $\langle d_{j,i}^{+} \rangle$ and $\langle d_{j,i}^{-} \rangle$, the power coefficients P_i, and the noise power σ^2. We assume that on average about one bit error is made for every symbol error, which is an excellent approximation for systems operating at very low probabilities of error with appropriate encoding [6].

Conditioning on the value of $a_{i,0}$, we have

$$\begin{aligned} P_e^i &= \sum_{x=1}^{L_i} \Pr\left(\text{Error}|a_{i,0} = \frac{2x-(L_i+1)}{L_i-1}\right) \\ &\quad \cdot \Pr\left(a_{i,0} = \frac{2x-(L_i+1)}{L_i-1}\right) \end{aligned} \tag{16}$$

$$\begin{aligned} &= \frac{1}{L_i} \Pr\left(\text{Error}|a_{i,0} = 1\right) + \frac{1}{L_i} \Pr\left(\text{Error}|a_{i,0} = -1\right) \\ &\quad + \frac{L_i - 2}{2L_i} \Pr\left(\text{Error}|a_{i,0} = \frac{+1}{L_i - 1}\right) + \frac{L_i - 2}{2L_i} \\ &\quad \cdot \Pr\left(\text{Error}|a_{i,0} = \frac{-1}{L_i - 1}\right) \end{aligned} \tag{17}$$

$$\begin{aligned} &= \frac{1}{L_i} \Pr\left(\psi_i + \phi_i + P_i d_{i,i}^{+}(0) < K_i + \frac{L_i - 2}{L_i - 1} P_i\, d_{i,i}^{+}(0)\right) \\ &\quad + \frac{1}{L_i} \Pr\left(\psi_i + \phi_i + P_i\, d_{i,i}^{-}(0) > K_i \right. \\ &\quad \left. + \frac{L_i - 2}{L_i - 1} P_i\, d_{i,i}^{-}(0)\right) + \frac{L_i - 2}{2L_i} \\ &\quad \cdot \left[1 - \Pr\left(K_i < \psi_i + \phi_i + \frac{1}{L_i - 1} P_i d_{i,i}^{+}(0) < K_i \right.\right. \\ &\quad \left.\left. + \frac{2}{L_i - 1} P_i\, d_{i,i}^{+}(0)\right)\right] \\ &\quad + \frac{L_i - 2}{2L_i}\left[1 - \Pr\left(K_i < \psi_i + \phi_i + \frac{1}{L_i - 1} \right.\right. \\ &\quad \left.\left. \cdot\ P_i d_{i,i}^{-}(0) < K_i + \frac{2}{L_i - 1} P_i\, d_{i,i}^{-}(0)\right)\right]. \end{aligned} \tag{18}$$

The $(L_i-2)/2$ positive "internal" symbols $\{1/L_i - 1, \cdots, L_i - 3/L_i - 1\}$ each have the same probability of error, as do the negative internal symbols $\{-1/L_i - 1, \cdots, -(L_i - 3)/L_i - 1\}$. This is because the distance between any two internal positive or negative symbols is equal. The "external" symbols $+1$ and -1 do not have the same probability of error as the internal symbols since there is only one symbol adjacent to each, instead of two for the internal symbols. K_i is the constant shift in the decision threshold due to DC-offset signals.

Collecting like terms in (18) gives the final expression for the probability of error

$$\begin{aligned} P_e^i &= \frac{1}{2}\left[\Pr\left(\psi_i + \phi_i + \frac{P_i\, d_{i,i}^{+}(0)}{L_i - 1} - K_i < 0\right)\right. \\ &\quad \left. + \Pr\left(-\psi_i - \phi_i - \frac{P_i\, d_{i,i}^{-}(0)}{L_i - 1} + K_i < 0\right)\right] \\ &\quad + \left(\frac{1}{2} - \frac{1}{L_i}\right)\left[\Pr\left(-\psi_i - \phi_i + \frac{P_i\, d_{i,i}^{+}(0)}{L_i - 1} + K_i < 0\right)\right. \\ &\quad \left. + \Pr\left(\psi_i + \phi_i - \frac{P_i d_{i,i}^{-}(0)}{L_i - 1} - K_i < 0\right)\right]. \end{aligned} \tag{19}$$

Following the moment generating function technique developed in [7], we can evaluate each of the probabilities of (19) using

$$\Pr\left(\alpha\psi_i + \beta\phi_i + \kappa_i < 0\right) = \int_0^{\infty} I_i(c + jz)\, dz \tag{20}$$

where $c > 0$ is chosen to speed the numerical evaluation of the integral and

$$I_i(s) = \frac{1}{\pi} \text{Re}\left\{s^{-1} \Psi_i(\alpha s) \Phi_i(\beta s) \exp\left(-s\kappa_i\right)\right\}. \tag{21}$$

$\Psi_i(s)$ and $\Phi_i(s)$ are the moment-generating functions of the random variables ψ_i and ϕ_i, and are given by

$$\Phi_i(s) = E(e^{-\phi_i s}) = \exp\left(\sigma_i^2 s^2/2\right) \tag{22}$$

$$\begin{aligned} \Psi_i(s) &= E(e^{-\psi_i s}) \\ &= \prod_{j=1}^{M} \prod_{\substack{k=-\infty \\ k \neq 0 \text{ if } j=i}}^{\infty} \frac{1}{L_j}\left[\sum_{x=1}^{L_j/2} \exp\left(\frac{2x-1}{L_j - 1} s P_j\, d_{j,i}^{+}(k)\right)\right. \\ &\quad \left. + \sum_{x=1}^{L_j/2} \exp\left(\frac{2x-1}{L_j - 1} s P_j\, d_{j,i}^{-}(k)\right)\right]. \end{aligned} \tag{23}$$

The last product can be truncated to those terms with significant values of $d_{j,i}^{+}$ and $d_{j,i}^{-}$.

In the preceding development, the intention is that we will be able to attain any given P_e^i by increasing the power coefficients P_i. Looking at (20), we note that if $\alpha\psi_i + \kappa_i < 0$ for some interfering data sequence, we will have $P_e^i > \frac{1}{2}\Pr(\alpha\psi_i + \kappa_i < 0)$ where the $\frac{1}{2}$ is the probability that the noise does not "help" the decision. Since ψ_i and κ_i are both proportional to the power coefficients, increasing their values will not reduce the probability of error. When this bit error rate (BER) floor is greater than the target BER for the system, we declare that an *outage* has occurred.

IV. Performance Results

We will examine the performance of various modulation schemes on both LOS and diffuse systems by averaging performance over an ensemble of experimentally determined channels. This will show both the appropriateness of modulation schemes for such systems and will also point out whether LOS or diffuse configurations are better if MSM is employed. Both a moderate (30 Mb/s) and a high (100 Mb/s) aggregate link rate are considered.

A. Modulation Schemes Considered

Each modulation scheme considered is based on either PAM for single-subcarrier (baseband) schemes or QAM for multiple-subcarrier schemes. We use the notation N-L-QAM or N-L-PAM to refer to a scheme utilizing N QAM (PAM) subcarriers, each of which has a symbol set size of L. We consider 1-L-PAM, 2-L-QAM, and 4-L-QAM. The potential benefits of MSM, which are reducing ISI, reducing the bandwidth requirement, and allowing multiple users access to the channel, do not increase substantially when more than four subcarriers are used, while the power inefficiencies of MSM (to be discussed) continue to increase with the number of subcarriers.

The unequalized PAM schemes we consider are 1–2-PAM and 1–4-PAM with rectangular transmit pulse shapes. It has been found [8], [9] that a five-pole Bessel filter with a 3-dB cutoff frequency of $0.6/T$ performs better on these multipath channels than a rectangular (integrate-and-dump) filter. We also consider the use of zero forcing decision feedback equalizers (ZF–DFE) due to the significant ISI. In this case, following [8] and [9], the cutoff frequency of the Bessel filter is chosen to be $0.45/T$.

A multiple-subcarrier QAM-based modulation scheme is formed by taking N independent QAM signals modulated to N different carrier frequencies $\{f_1, f_2, \cdots, f_N\}$. N-QAM is thus described by pulse shapes defined as

$$\begin{aligned} x_m(t) &= p(t)\cos(2\pi f_m t + \phi_m) \\ y_m(t) &= p(t)\sin(2\pi f_m t + \phi_m). \end{aligned} \tag{24}$$

The pulse shape $p(t)$ will be a unit-energy rectangular pulse of duration T or a root-raised-cosine (RRC) pulse of excess bandwidth (EBW) chosen to be 50% or 100%.

Clipped N-4-QAM is also of the form (24), but only rectangular pulses are considered. The average optical power of clipped N-4-QAM is

$$P_{\text{clip}} = \frac{2}{\pi\sqrt{T}} \sum_{i=1}^{2M} P_i \tag{25}$$

which is $\sqrt{8}/\pi$ times the power required by DC-offset 4-QAM with the same number of subcarriers. Hence, clipped 4-QAM will require 0.46 dB less average optical power on the ideal channel.

A modification of N-L-QAM which is used to reduce the required frequency spacing of subcarriers is "staggering." Here the pulse shapes are given by (26), shown at the bottom of the page.

B. Power Requirement Evaluation

Some factors affecting the transmit power requirement apply to both single-carrier and multiple-subcarriers systems. The Gaussian noise power of the channel provides the fundamental impediment to reliable communication and ISI reduces the noise immunity of the signal and may also cause a BER floor. Also, multilevel modulation schemes will suffer reduced power efficiency relative to binary modulation schemes due to constellation crowding. There are additional factors that influence the power required by MSM schemes. Increasing the number of subcarriers used to transmit a given total bit rate will lead to a greater DC-offset requirement. For systems that use quadrature phases to transmit two data streams at the same subcarrier frequency, there is cross-subcarrier interference. There is also the possibility of adjacent-carrier interference from signals at other subcarrier frequencies if the sidelobes of the subcarriers overlap. Finally, the essentially lowpass nature of the channel introduces another source of power loss, as subcarriers using higher frequencies suffer greater channel attenuation.

The choice of the transmit and receiver pulse shapes will affect the relative importance of ISI, adjacent-subcarrier interference, and cross-subcarrier interference. Both rectangular and RRC pulse shapes are considered. They represent the typical examples of satisfying the generalized Nyquist criterion [6] through time separation (rectangular) or frequency separation (RRC). The corresponding matched receive filters are rectangular and RRC pulses. Rectangular pulses may permit adjacent-subcarrier interference, while RRC pulses do not. We address the problem of high-frequency channel attenuation by using multilevel modulation and/or subcarrier staggering to reduce the bandwidth required by the transmitted signal. Multilevel modulation introduces constellation crowding,

$$\begin{pmatrix} x_{(2m)}(t) & y_{(2m)}(t) \\ x_{(2m-1)}(t) & y_{(2m-1)}(t) \end{pmatrix} = \begin{pmatrix} p(t)\cos(2\pi f_{(2m)}t) & p(t-T/2)\sin(2\pi f_{(2m)}t) \\ p(t-T/2)\cos(2\pi f_{(2m-1)}t) & p(t)\sin(2\pi f_{(2m-1)}t) \end{pmatrix}. \tag{26}$$

while staggering re-introduces adjacent-subcarrier interference to systems using RRC pulses.

Transmission over a channel $h(t)$ results in two effects, namely path loss and multipath distortion. In this paper, we are interested in the extent to which, for a given received average optical power, multipath distortion increases the BER. Accordingly, we normalize all channels to have 0 dB of optical path loss by taking $\int_{-\infty}^{\infty} h(t)\,dt = 1$. To compare the average-power efficiency of modulation schemes, let us define a function $P(\mathrm{BER}, h(t), N_0, \mathrm{MS})$ as the average optical transmitted power required when using the modulation scheme (MS) to achieve a BER over the channel with impulse response $h(t)$ in the presence of additive white Gaussian noise (AWGN) of power-spectral density N_0. Then the *normalized power requirement* is $P_{\mathrm{avg}}/P_{\mathrm{OOK}} = P(\mathrm{BER}, h(t), N_0, \mathrm{MS})/P(\mathrm{BER}, \delta(t), N_0, \mathrm{OOK})$, which can be thought of as a power penalty for the channel and modulation scheme compared to 2-PAM (OOK) on a nondistorting channel. In this paper, we use a target BER of 10^{-9} throughout and we require that this BER is achieved in each subcarrier rather than simply that the aggregate signal attain the target BER.

From [4], $P_{\mathrm{OOK}} = \sqrt{N_0 R_b}\,Q^{-1}(\mathrm{BER})$, where R_b is the bit rate. We calculate P_{avg} by estimating the power coefficients P_i, evaluating the BER achieved, and then providing a new estimate of the power coefficients. In this section, the power coefficients P_i are constrained to be equal under the assumption that no adaptation to the channel frequency response is done. The calculation is iterated until the error rates are within a tolerance range of the required BER. The calculation has been found to be accurate to within 0.01 dB in those cases that can easily be verified.

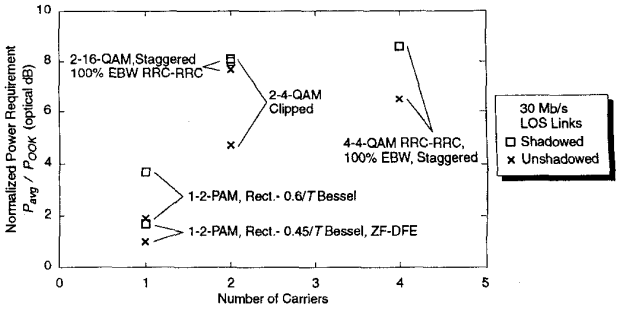

(a)

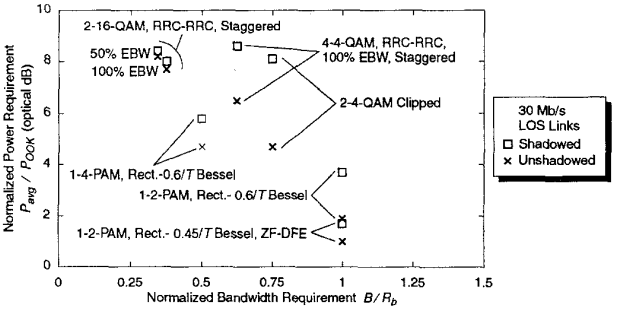

(b)

Fig. 3. Optical average-power requirements of several MSM and PAM schemes for 30-Mb/s LOS links. The reference (0 dB) is for an OOK link on a distortionless channel. "N-4-QAM" and "N-16-QAM" refer to N 4-QAM or 16-QAM subcarriers, respectively. "1-L-PAM" means a single L-PAM subcarrier. "RRC–RRC" means that both transmitter and receiver filters are RRC, with the EBW stated. "Rect.-K/T Bessel" means that the transmit pulse is rectangular and the receive filter is a five-pole Bessel filter with 3-dB cutoff frequency K/T, where T is the symbol time. "ZF–DFE" indicates that zero-forcing decision feedback equalization is used. "Staggered" refers to the time-staggering of I and Q carriers. "Clipped" refers to half-wave rectification of each 4-QAM subcarrier. The power requirements are averaged over 30 LOS unshadowed, 20 LOS shadowed, 21 diffuse unshadowed, and 17 diffuse shadowed channels.

C. Results

We compare modulation-scheme performance in terms of two parameters: the number of subcarriers, and the bandwidth requirement. The number of carriers affects the required speed of the demodulation electronics, and also influences the multipath immunity of the signal. The bandwidth requirement B is the width of the frequency range from DC to the first null of the highest-frequency subcarrier, and it is normalized by the total transmitted bit rate R_b. This is a measure of the electrical bandwidth required to pass the electrical signal resulting from direct detection.

1) 30-Mb/s LOS Links: Graphs of the average optical power penalty as a function of the number of carriers and the bandwidth requirement for 30-Mb/s LOS links are shown in Fig. 3. The best two-subcarrier MSM schemes are clipped 2–4-QAM and staggered 2–16-QAM with 100%-EBW RRC–RRC pulses. Although the latter is 0.1 dB better on shadowed channels, clipped 4-QAM is 3.0 dB better on unshadowed channels. This difference is due to the much better responses of LOS unshadowed channels: on such channels neither modulation experiences significant distortion and so the inherently more power-efficient clipped 4-QAM performs better. On the more distorting LOS shadowed channels, 2–16-QAM is more immune to distortion, and this more than makes up for its initially poor power efficiency. Increasing to four subcarriers, we find that staggered 4–4-QAM with 100%-EBW RRC–RRC pulses is worse than clipped 2–4-QAM by 1.8 dB on unshadowed channels and 0.5 dB on shadowed channels. In comparison to 2-PAM with ZF–DFE and 0.45/T Bessel filter, we give up about 5 dB by using two carriers and 6 dB by using four carriers.

There is a steady increase in power penalty as the bandwidth requirement is decreased. The best modulation schemes in terms of bandwidth requirement are 2-PAM Bessel, 4-PAM Bessel, and staggered RRC 2–16-QAM. Relative to 2-PAM, which requires 1 Hz/b/s, 4-PAM Bessel requires 0.5 Hz/b/s and 2 dB more average optical power, staggered 100%-EBW 2–16-QAM requires 0.38 Hz/b/s and 4.0 dB more average optical power, and staggered 50%-EBW 2–16-QAM requires 0.34 Hz/b/s and 4.3 dB more average optical power.

2) 30-Mb/s Diffuse Links: Graphs of the average optical power penalty as a function of the bandwidth requirement and the number of carriers for 30-Mb/s diffuse links are shown in Fig. 4. The power penalty for increasing the number of carriers is not as large as for LOS links, as we lose only 3 dB and 4.5 dB of power efficiency for two and four subcarriers,

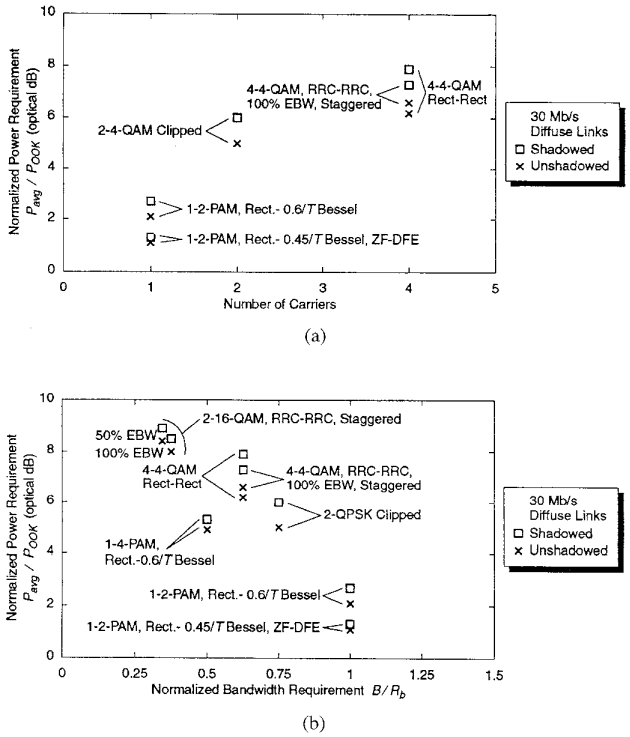

Fig. 4. Optical average-power requirements of several and PAM schemes for 30-Mb/s diffuse Links. The notation is the same as for Fig. 3.

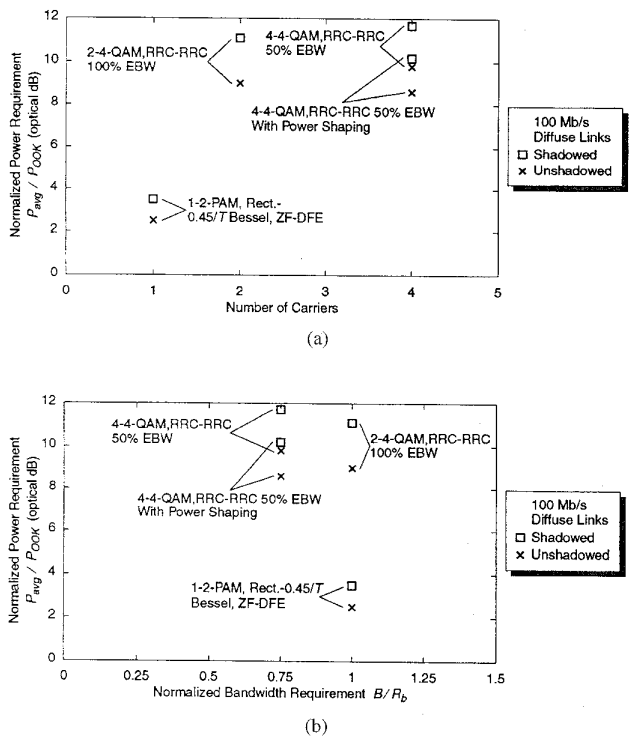

Fig. 5. Optical average-power requirements of several MSM and PAM schemes for 100-Mb/s diffuse links. The notation is the same as for Fig. 3. Power shaping refers to individual adjustment of each subcarrier power coefficient to compensate for the channel frequency response.

respectively. These results are for clipped 2–4-QAM and staggered 100%-EBW RRC–RRC 4–4-QAM.

There is a steady increase in power penalty as the bandwidth requirement is decreased. The best modulation schemes here are 2-PAM Bessel, 4-PAM Bessel, and DC-offset RRC 2–16-QAM. 4-PAM Bessel requires 0.5 Hz/b/s and 3 dB more average optical power than 2-PAM. DC-offset 50%-EBW 2–16-QAM requires 0.41 Hz/b/s, but is about 6 dB worse than 2-PAM.

3) 100-Mb/s LOS Links: At 100 Mb/s, there are no modulation schemes free of outages for all LOS shadowed and LOS unshadowed channels, and so no plots of average optical power penalty are possible. Unequalized 2-PAM with a $0.6/T$-Bessel filter suffered outages on all 20 LOS shadowed channels, and on three of 30 LOS unshadowed channels. The best two and four subcarrier scheme is DC-offset 4-QAM with 100%-EBW RRC–RRC pulses. Both 2–4-QAM and 4–4-QAM are free of outages on LOS unshadowed channels and had only one outage out of 20 shadowed channels.

4) 100-Mb/s Diffuse Links: Almost all modulation schemes operating at 100 Mb/s experience outages on some diffuse channels. Unequalized 2-PAM with a $0.6/T$-Bessel filter suffers outages on eight of 17 diffuse shadowed channels, and on three of 21 diffuse unshadowed channels. The schemes free of outages are the DC-offset RRC 4-QAM schemes, which maintain complete frequency separation between adjacent carriers. The power efficiencies of these schemes and of equalized 2-PAM are shown in Fig. 5. The loss of power efficiency is significant: about 7 dB for 2–4-QAM 100%-EBW RRC–RRC and slightly more for 4–4-QAM 50%-EBW RRC–RRC.

V. Enhancement Techniques

We consider two techniques for improving the performance of MSM: carrier selection and power shaping. The goals are to reduce the number of channels experiencing an outage and to reduce the average power penalty.

Carrier selection is done by looking at the most promising possible frequency assignments for the N subcarrier frequencies. For rectangular-pulse MSM, this is done for all subcarriers jointly to account for the effect of each subcarrier on its neighbors. For RRC-pulse MSM, we look at each possible subcarrier frequency separately and pick the best N frequencies. DC-offset 2–4-QAM with rectangular pulses at 100 Mb/s experiences outages on 23 of 88 channels without carrier selection, but only on four of 88 with carrier selection. Neither LOS nor diffuse channels were free of outages, however. The improvement was less significant for 4–4-QAM, with the number of channel outages reducing from 31 to 24 with carrier selection. The effect of carrier selection on DC-offset 4–4-QAM using 50%-EBW RRC pulse shapes is less significant. In each case, using the minimum possible set of subcarrier frequencies $(3/4T)\{1;3;5;7\}$ provides the best performance. There are several instances in which there is a relative null at one subcarrier frequency, but in all cases moving all the subsequent subcarriers to higher frequencies beyond the null makes the eventual performance worse.

We also consider the power efficiency improvement that can be obtained by allowing the P_i to take on different values for each subcarrier. We wish to adjust the P_i so that

each subcarrier achieves the same BER target. On diffuse unshadowed channels, the average optical power penalty is reduced from 9.8 dB without power shaping to 8.6 dB with power shaping. This compares to the average performance of ZF–DFE equalized 2-PAM of 2.5 dB. On diffuse shadowed channels, the average optical power penalty is reduced from 11.7 dB without power shaping to 10.2 dB with power shaping, and where the ZF–DFE 2-PAM penalty is 3.5 dB.

VI. Application to Multi-User Systems

The preceding models and results make the assumption that there is a single transmitter and a single receiver, and one wishes to send information from the transmitter to the receiver. A simple extension would be to allow for N_t transmitters. Transmitter i would send signal $X_i(t)$ and the received signal would be (1)

$$Y(t) = \sum_{i=1}^{N_t} (X_i(t) \otimes h_i(t)) + n(t) \tag{27}$$

where $h_i(t)$ is the impulse response between transmitter i and the receiver. Some structure would need to be imposed on the X_i if the receiver is to correctly demodulate each transmission. This could easily be done by having all transmitters use the same MSM format, but with $P_i = 0$ for transmitter j when $i \neq j$. Using QAM as an example, we would have (7)

$$X_i(t) = DC_i + \sum_{k=-\infty}^{\infty} P_i\{u_{i,k} \cdot x_i(t - kT) + v_{i,k} \cdot y_i(t - kT)\}. \tag{28}$$

An obvious alternative would be to use time-division multiplexing. In this case, the transmitted signals would be (11)

$$X_i(t) = DC_i + \sum_{k=-\infty}^{\infty} P_i \cdot a_{i,k} A(t - kN_tT - iT). \tag{29}$$

To the extent that the different channels $\{h_i(t), i = 1, \cdots, N_t\}$ are similar, the power comparison between a single-transmitter MSM system and a single-transmitter PAM system will apply exactly to the power comparison between a multiple-transmitter MSM system to a multiple-transmitter TDM system. The power comparisons will tend to hold even when there are variations in the response for different transmitters, since channels that are poor for PAM are usually poor for most subcarriers as well.

The power comparison could be further evaluated given a model for the variation of $h(t)$ with position and a model for the pattern of user traffic.

VII. Conclusions

For LOS and diffuse systems in which shadowing is a concern, MSM schemes perform better on diffuse systems (as do PAM schemes) in terms of both power efficiency and fraction of channels experiencing an outage. Although LOS unshadowed links provide the best overall performance, LOS shadowed links are severely degraded. The power efficiency gap between diffuse shadowed links and diffuse unshadowed links is smaller.

At 100 Mb/s, the only schemes that provide for outage-free unequalized operation are DC-offset 4-QAM with RRC pulses. The strict frequency-separation of the DC-offset schemes avoid the severe cross-subcarrier interference suffered by schemes using staggering and clipping.

When classified by the number of carriers used, many different modulation schemes have the best overall average power penalty in the four channel categories considered, at both the 30 Mb/s and 100 Mb/s data rates considered. Root-raised-cosine pulses are preferable in most instances to rectangular pulses. 4-QAM augmented by the techniques of staggering and clipping outperforms the simple DC-offset schemes at 30 Mb/s.

MSM can provide improvements in receiver bandwidth required relative to 2-PAM, at the expense of power efficiency. At 30 Mb/s, the use of either 4-PAM or 2–16-QAM with staggering reduces the bandwidth required by a factor of 2.0 for 4-PAM, and a factor of 2.9 for 2–16-QAM, with losses in power efficiency of 2 dB and 4 dB, respectively.

MSM schemes offer advantages over single-carrier modulation schemes in several respects. They are more robust at high total bit rates if equalization at the receiver is not an option. They provide a flexible method of allowing multiple simultaneous users of the channel, without requiring synchronization of the transmitters, and without forcing each receiver to demodulate the signals destined for others. And finally, they can reduce the electrical bandwidth requirement of the receiver.

The primary disadvantage of MSM schemes is that they are less power-efficient than single-carrier modulation schemes. The power penalty increases with the bandwidth efficiency, the number of subcarriers employed, and the aggregate rate required. The best multiple-subcarrier modulation schemes require between 3 dB and 7 dB more optical power than equalized single-carrier modulation schemes.

References

[1] F. R. Gfeller and U. H. Bapst, "Wireless in-house data communication via diffuse infrared radiation," *Proc. IEEE*, vol. 67, pp. 1474–1486, Nov. 1979.

[2] J. M. Kahn, W. J. Krause, and J. B. Carruthers, "Experimental characterization of nondirected indoor infrared channels," *IEEE Trans. Commun.*, vol. 43, pp. 1613–1623, Feb./Mar./Apr. 1995.

[3] J. M. Kahn, J. R. Barry, M. D. Audeh, J. B. Carruthers, W. J. Krause, and G. W. Marsh, "Non-directed infrared links for high capacity wireless LANs," *IEEE Personal Commun. Mag.*, vol. 1, May 1994.

[4] J. R. Barry, *Wireless Infrared Communications*. Boston: Kluwer, 1994.

[5] T. E. Darcie, "Subcarrier multiplexing for lightwave networks and video distribution systems," *IEEE J. Select. Areas Commun.*, vol. 8, pp. 1240–1248, Sept. 1990.

[6] E. A. Lee and D. G. Messerschmitt, *Digital Communication*, 2nd ed. Boston: Kluwer, 1994.

[7] C. W. Helstrom, "Calculating error probabilities for intersymbol and cochannel interference," *IEEE Trans. Commun.*, vol. COM-34, pp. 430–435, May 1986.

[8] J. B. Carruthers, "Performance and design of multiple-subcarrier modulation schemes for wireless indoor infrared LAN's," M.S. thesis, University of California at Berkeley, Dec. 1993.

[9] W. J. Krause, "Experimental characterization of nondirective indoor infrared channels," M.S. thesis, University of California at Berkeley, Dec. 1992.

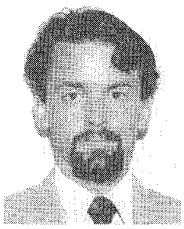

Jeffrey B. Carruthers (S'80–M'84) received the B.Eng. degree in computer systems engineering from Carleton University, Ottawa, Canada, in 1990, and the M.S. degree in electrical engineering from the University of California at Berkeley, in 1993, where he is working toward the Ph.D. degree.

He joined Bell-Northern Research, Ottawa, where he worked on the development of SONET products until 1991. His research interests are in broadband wireless communications.

Joseph M. Kahn (M'90) received the A.B., M.A., and Ph.D. degrees from the University California at Berkeley, all in physics, in 1981, 1983, and 1986, respectively.

From 1987 to 1990, he was a Member of Technical Staff in the Lightwave Communications Research Department of AT&T Bell Laboratories at the Crawford Hill Laboratory, Holmdel, NJ, where he performed research on multigigabit- per-second coherent optical fiber transmission systems and related device and subsystem technologies. He demonstrated the first BPSK-homodyne optical fiber transmission system, and achieved world records for receiver sensitivity in multigigabit-per-second systems. In 1990, he joined the faculty of University of California at Berkeley, where he is now an Associate Professor with the Department of Electrical Engineering and Computer Sciences. His research interests include optical fiber communication networks and transmission systems, local-area networks using free-space optical links, and optical interconnects in digital systems.

Dr. Kahn is a recipient of the National Science Foundation Presidential Young Investigator Award. He is serving currently as a technical editor of *IEEE Personal Communications Magazine.*